Pakistan Journal of Science (Vol. 75 No. 3 September, 2023)

APPLICATION OF MODIFIED BIOCHAR FOR HEXAVALENT CHROMIUM SORPTION FROM WATER

M. B. Shakoor[1*], I. Masood ul Hasan[2,3], N. A. Abbasi[1], M. Majid[1], S. R. Ahmad[1], A. Sadaf[1], M. Hassan Shakoor[4] and M. Aslam[1],

[1]College of Earth and Environmental Sciences, University of the Punjab, Lahore 54000, Pakistan
[2]key Laboratory of Comprehensive and Highly Utilization of Salt and Lake Resources, Qinghai Institute of Salt and Lakes, Chinese Academy of Sciences, Xining, 810008, China
[3]Institute of Soil and Environmental Sciences, University of Agriculture Faisalabad, Faisalabad, 38040, Pakistan
[4]Department of Chemistry, Riphah International University, Faisalabad, Pakistan
Corresponding author email:[*]: bilalshakoor88@gmail.com

ABSTRACT: In this study, we prepared novel mosambi peel biochar (M–BC) and KOH-based engineered mosambi peel biochar (KOH–M–BC) and used for the removal of hexavalent chromium (Cr(VI)) from water. Successful modification with KOH showed the highest Cr(VI) sorption at pH 4 (118.7 mg/g (98.5%)) on KOH–M–BC compared to M–BC (108.6 mg/g (90%)). The experiments related to effect of other major sorption parameters suggested that the maximum sorption was observed at 120 mg/L initial Cr(VI) concentration, 0.9 g/L sorbent dose and 4 hour contact time. The Langmuir ($R^2=0.98$) isotherm model provided the best fitted data for both sorbents, notably for KOH–M–BC indicating the monolayer sorption. The pseudo-second-order model ($R^2=0.99$) well-described the kinetics of Cr(VI) sorption on both sorbents. The FTIR results shows that the surface functional groups such as OH, C=O and COO– contributed to Cr(VI) sequestration by the both biochars. The SEM images showed the porous surface of KOH–M–BC which provided numerous sites for Cr(VI) attachment on biochar. The presence of Cr(VI) onto biochar after adsorption was also confirmed by XPS analysis. This findings of this research highlighted the importance of surface modification with alkali (KOH) and a potentially viable, green and cost-effective sorbent for Cr(VI removal from water.

Keywords: Biochar, Alkali, Modification, sorption, water treatment.

(Received 28.07.2023 Accepted 14.09.2023)

INTRODUCTION

Rapid industrialization, urbanization, environmental contamination and ecological factors are some key issues that lead to the expansion of many human health problems. Chromium (Cr) is directly discharged to water sources from industries (Leather tanning, textile) that are allocated to humans for drinking thereby causing serious consideration for scientists (Din *et al*., 2021; Ai *et al*., 2023). Hexavalent chromium Cr(VI) is an inorganic form of Cr which is highly hazardous for humans because it is highly soluble, teratogenic, mobile and carcinogenic in nature (Scharf *et al*., 2014; Ai *et al*., 2023). Therefore, finding reliable and green strategies for the sorption of Cr(VI) has become an essential requirement to protect people from Cr(VI) poisoning.

Various removal technologies such as ion exchange, electrochemical precipitation, reduction method, cementation, evaporation, solvent extraction, membrane separation, ultrafiltration, electro-dialysis and biosorption are used for Cr(VI) containing water treatment (Park *et al*., 2008; Basu *et al*., 2014; Peng and Guo, 2020). However, these treatment technologies are expensive, require energy, laborious and not efficient for smaller concentrations. Biochar (BC) is carbonaceous material with a high surface area, large pore size, and easily available low-cost biomaterial with high surface functional groups (Masood ul Hasan *et al*., 2022). Although, BC is an attractive and effective material for the adsorption of heavy metals but organic debris, indigenous inorganics and the presence of impurities decrease the efficiency. A post-treatment of BC is considered as an effective way to increase the sorption capacity. Typically chemical and physical methods not only increase the pore size but also significantly improve the surface area of BC. However, low yield, chemical cost and weight loss decrease the economic feasibility of BC. Therefore surface modification is considered as most effective technique than harsh surface activation.

Surface modification is simple post-engineering method which showed high sorption capacity for heavy metals removal than activation. For example surface modification with oxidizing agents (e.g $Fe(NO_3)_3$, air, HNO_3 and H_2O_2) is a typical modification method which showed increased sorption from 1.04 mg/g to 22.82 mg/g for lead (Pb) by using H_2O_2 as oxidizing agent on raw BC surface (Xue *et al*., 2012). Metal salt soaking, alkali and acid modification is another rising method for pollutant removal from water. Regmi *et al*., (2012) stated that BC treated with high alkali (2N) showed maximum removal for copper (34 mg/g) and cadmium (31 mg/g), respectively. However, some disadvantages are also reported related to this method such as weight loss and high consumption of chemicals for BC modification. Therefore, economically feasible and high performance based BC for sorption processes is a need of the time.

To the best our knowledge, no study is directed to evaluate the influence of novel mosambi peel biocahr (M–BC) and alkali based-KOH engineered mosambi peel biocahr (KOH–M–BC) for Cr(VI) removal from water. This is important because surface modification with alkali is simple and possible substitute of harsh surface activation process that could provide various functional groups during sorption of Cr(VI) by BC. In the current study, newly prepared M-BC and KOH-M-BC were compared for Cr(VI) removal from water under varying environmental conditions. In addition, isotherm and kinetic modeling as well as SEM-EDS, FTIR and XPS analyses were performed to evaluate the Cr(VI) sorption mechanism and to analyze the surface properties of biochars.

MATERIALS AND METHODS

Reagents and chemicals: All the chemicals which were used in this experiment including: potassium dichromate ($K_2Cr_2O_7$), nitric acid (HNO_3), potassium hydroxide (KOH), hydrochloric acid (HCL) and sodium hydroxide (NaOH) were of analytical grade. Distilled water (DW) was used in the preparation of Cr(VI) stock and working solutions by dissolving appropriate amount $K_2Cr_2O_7$. Nitric acid (HNO_3) (2%) was used to wash plasticware and glassware prior to use for experimental purpose. Solution pH was maintained by using 0.1 M HCl and NaOH.

Preparation of sorbent

Mosambi peel biochar: Mosambi peel biomass (organic waste) was collected from local market in Faisalabad (Pakistan), sun-dried, oven-dried, grounded and sieved by using 2 mm mesh sieve. Mosambi peel biochar (M–BC) was prepared under strictly anoxic condition at 550 °C in a muffle furnace.

KOH engineered mosambi biochar: The M–BC is used to synthesis KOH engineered mosambi peel biocahr (KOH–M–BC). Briefly, 28.05 g of KOH, 15 g of M-BC was dissolved in 25 ml of DW followed by slow stirring for 2 h at room temperature. Upper layer was removed and then the slurry type material followed continuous stirring and oven dried for 24 h at 40 °C. This newly prepared material (KOH–M–BC) was stored for further experiments.

Batch sorption: All the batch sorption experiments were conducted using 50 mL polyvinyl reaction tubes (20±2°C) with 0.1 M NaCl as background electrolyte and 2 h equilibrium time calculated from kinetic batch study (see below).

Influence of pH (3–8), initial Cr concentration (5–200 mg/L), contact time (1min–4 h) and competing ions (SO_4^{2-} and PO_4^{3-}) were examined for Cr(VI) removal from water by M–BC and KOH–M–BC sorbents. Kinetic study was performed at different time interval (0.016 to 24h) to determine the effect of contact time on Cr(VI) sorption at optimum pH. The suspension pH was adjusted with 0.01 M HCl and NaOH for all sorption experiments. The optimum sorbent dose of 0.9 g/L was used to check the optimum initial Cr concentration required for all sorption experiment.

In all sorption experiments, solution was subjected to end-to-end agitation for 2 h followed by centrifugation at 4000 rmp for further process. The supernatant solution was separated with 0.45 µm syringe filter and stored at stored at 4 °C for total Cr analysis by atomic absorption spectrometer (Perkin Elmer AAnalyst 800, USA)

The % removal of Cr was calculated by following the equation (Eq. 1)

$$\%\ \text{Cr removal} = \frac{Co - Ce}{Co} \times 100 \qquad (1)$$

Where C_o, stands for initial Cr concentration, C_e stand for the final Cr value in the solution. While sorption capacity (q_e) of Cr is calculated by (Eq. 2)

$$\text{qe} = \frac{(Co - Ce)V}{m} \qquad (2)$$

Where, m stands for BC weight (g), V is the volume of solution (L), C_o and C_e are mentioned above (Eq. 1)

Sorption isotherm and kinetic modeling: Isotherm models (Langmuir, and Freundlich) were applied using Cr(VI) sorption studies data. Rate of sorption was evaluated by using Cr(VI) sorption on both sorbents using pseudo-first and second-order models (Prasad *et al*., 2012).

Quality control and assurance for Cr(VI) analysis: The quality of total Cr analysis was examined by running blank reagents (no sorbents and no Cr(VI)). After every 10 samples, known (reference) Cr concentration samples was analyzed for analytic assurance. The 2.5% residual deviation (RSD) was used for Cr analysis.

RESULTS AND DISCUSSION

Influence of pH: Chemical state of Cr(VI) was affected by aqueous media pH. This is determined by the functional groups present on adsorption sites and different charges on prepared sorbents surfaces (Alghamdi *et al*., 2023). Therefore influence of pH (3–8) in batch sorption was determined for Cr(VI) sorption.

Figure 1a,b showed the sorption capacity of M–BC and KOH–M–BC sorbents. Results show that Cr(VI) sorption is a pH dependent as pH increases from 4 to 8, sorption of Cr(VI) gradually decreases.

Among our sorbents, maximum Cr(VI) sorption was achieved at pH 4 that is 118.7 mg/g (98.5%) followed by 112.7 mg/g, 105.6 mg/g, 104.6 mg/g, 101.1 mg/g at pH 5, 6, 7 and 8, respectively, by KOH–M–BC. In contrast M-BC also show maximum Cr(VI) sorption at pH 4 that was 108.6 mg/g (90%) followed by 105.1 mg/g, 103.1 mg/g, 99.6 mg/g, 94.12 mg/g at pH 5, 6, 7 and 8, respectively.

This high sorption at low pH (4) could possibly be due to easy protonation and attraction of negative charges of Cr species, as Cr(VI) present in different stable form such as $Cr_2O_7^{2-}$, $HCrO_4^{-}$ at < pH 6 and CrO_4^{2} at pH> 6 (Zhao *et al*., 2017). Another possible reason is competition between Cr(VI) species and negatively charged –OH ions (from biochar) for sorption sites. At lower pH functional groups from KOH–M–BC become protonated and contribute towards the $Cr_2O_7^{2-}$ and $HCrO_4^{-}$ sorption on surface by electrostatic attraction and thus showed high sorption (98.5%) (Qu *et al*., 2019; Qu *et al*., 2021). However, decrease at higher pH (4–8) could be due to electrostatic repulsion of both negatively charged sorbents to anions Cr(VI) (Hu *et al*., 2020).

Influence of contact time on Cr(VI) sorption: Contact time is another important parameter used to calculate optimum time needed for the biosorption of Cr(VI) on sorbent surface. Our results demonstrated that as time increased, sorption of Cr(VI) also showed an increasing trend. Maximum Cr(VI) sorption was found at 4 hr (240 min) 119.8 mg/g (96%) on KOH–M–BC and 114.2 mg/g (91%) M–BC surface (Figure 1c). This could possibly when Cr(VI) was attached on the binding sites (after 4 hr), sorption kinetics significantly decreased until the rate of sorption became equal to rate of desorption.

Influence of initial Cr(VI) concentration on Cr(VI) sorption: Initial concentration produce driving force to transfer ions on sorbent surface from liquid solution so considered as another important parameter in sorption study (Khalil *et al*., 2018). In this study, we used different concentration for Cr(VI) ions (10-200 mg/L). Gradual increases was noted with maximum sorption of Cr(VI) at 120 mg/L on M–BC (190.35 mg/g) and KOH–M–BC (196.5 mg/g) surface (Figure 2a). The adsorption was minimum at low initial concentration and after 120 mg/L initial concentration, the adsorption rate of Cr(VI) again started to decline. This shows that significant competition between sorption sites and Cr(VI) ions helps the sorption until equilibrium point (Kokab *et al*., 2021). It is noteworthy that after equilibrium point increasing initial Cr(VI) had negligible or no effect on overall sorption process by M–BC and KOH–M–BC sorbent.

Influence of anions on Cr(VI) sorption: Industrial water contains many harmful cation and anions species which can affect the heavy metal uptake during sorption process (Kokab *et al*., 2021). Figure 2b shows the influence of competing ions on Cr(VI) sorption by M–BC and KOH–M–BC. The maximum reduction in Cr(VI) removal was noted on KOH–M–BC (86%) and M–BC (82%) in the presence of SO_4^{-2} while presence of PO_3^{-} showed less reduction of Cr(VI) removal about 88 and 85 % on KOH–M–BC and M–BC surface, respectively (Figure 2b). Our result demonstrated that both anions have significant influence in the reduction of Cr(VI) removal by M–BC and KOH–M–BC.

Kinetic modeling: Rate of Cr(VI) sorption was evaluated by kinetic modeling. Kinetics data were fitted to non-linear kinetic models (pseudo-first-order, pseudo-second-order) to describe the mononuclear and binuclear sorption. Table 1 shows the kinetic model parameters for Cr(VI) sorption on M–BC and KOH–M–BC surface.

Results revealed that R^2 value for pseudo-second-order is higher (R^2 = 0.99) as compared to pseudo-first-order (R^2 = 0.76) for M–BC. The greater, R^2 value for pseudo-second-order (R^2 = 0.99) as compared to pseudo-first-order (R^2 = 0.83) for KOH–M–BC was also reported. The calculated q_e value is also higher for pseudo-second-order (76 and 50 mg/g) as compared to pseudo-first-order (7.94 and 11.74 mg/g) on M–BC and KOH–M–BC surface, respectively. Overall, our results explain that the Cr(VI) sorption on M–BC and KOH–M–BC occurred due to chemisorption process which involved the interaction between surface functional groups and Cr oxyanions (Khalil *et al*., 2020).

Isotherm modeling: Isothermal models namely Freundlich and Langmuir models were applied for further evolution of nature of Cr(VI) adsorption on both sorbent surface.

The R^2 value for the Freundlich model was 0.80 for Cr(VI) sorption at M–BC and 0.78 at KOH–M–BC surface. The Q_F value of M–BC for Cr(VI) sorption was 1.82 $mg^{1-n}\,g^{-1}\,L^n$ and 1.83 $mg^{1-n}\,g^{-1}\,L^n$ for KOH–M–BC. The values of n of M–BC for Cr(VI) and KOH–M–BC were > 1 indicating favorable sorption for Cr(VI) (Belachew and Hinsene, 2019). In the case of Langmuir Isotherm, higher R^2 value (0.98) for both sorbents were. The higher Q_L value for Cr(VI) sorption on KOH–M–BC was noted compared to M–BC (Table 2). Langmuir model indicated higher values of R^2 (0.98) as compared to the Freundlich model for Cr(VI) sorption which explained the formation of monolayer on homogenous surface by physical-chemical sorption of Cr(VI) (Campos *et al*., 2019).

Overall our isotherm modeling results indicated that Langmuir model is the best fitted model for Cr(VI) sorption on both biochars.

SEM-EDS: The surface morphology of M–BC and KOH–M–BC are shown in SEM images (Figure 3a, b). It was observed that M–BC surface had continuous rough and fluffy surface (Figure 3a). The KOH modification of BC resulted in porous and highly wrinkled surface that significantly improved the number of micropores on KOH–M–BC surface (Figure 3b) (Zhang *et al*., 2018). Additionally, the porous surface structure of KOH–M–BC provides facilitation between BC and Cr(VI) ions in the solution thereby increasing the adsorption of Cr(VI) by surface attachment or electrostatic reactions (Khalil *et al*., 2018).

The SEM-EDS spectra (before adsorption) of M–BC and KOH–M–BC (Figure 4a,b) showed elements such as C, O, Na, Mg and Al were detected on M–BC surface while modified biochar (KOH–M–BC) showed C, O, Si, S and Cl as prominent ions.

XPS analyses: The surface chemical composition of M–BC and KOH–M–BC (Figure 5) was evaluated using XPS. The atomic C1s (76.1%) and O1s (21.6%) were observed from XPS results before adsorption and Cr(VI) appeared after adsorption on M–BC surface. This atomic % decreased after adsorption with presence of Cr (C1s (72.1%), O1s (19.0%) and Cr 2p3 (7.1%)) at M–BC surface (Figure 5a,c). The atomic % in KOH–M–BC shows that C1s (67.4%) and O1s (27.6%) were present before adsorption and Cr(VI) appeared after adsorption. This atomic % decreased after adsorption with presence of Cr (C1s (62.2%), O1s (23.1%) and Cr 2p3 (9.9%), respectively) at KOH–M–BC surface was noted (Figure 5b,d). Furthermore, KOH–M–BC showed relative higher Cr percentage as compared to M-BC thus proving that KOH treatment of biochar successfully enhanced the performance of biochar. The C1s XPS spectra could be assigned to C–C/C–H, C–O, C=O and C=O–O which were responsible for Cr(VI) adsorption by both sorbents (Zhang *et al*., 2018). It is important to note that there was no significant change in species before and after adsorption but relative atomic % content changed on both prepared biochar-based materials. The O1s spectra results indicated that binding energy was slightly shifted to lower energy region after adsorption showing that this change is due to Cr(VI) adsorption at M–BC and KOH–M–BC surface (Zhang *et al*., 2018; Kokab *et al*., 2021).

Fourier transform infrared spectroscopy (FTIR) for surface characterization: Fourier transform infrared (FTIR) spectroscopy is a promising technique to evaluate the surface functional groups, since every functional group have different stretching and bending energies (Masood ul Hasan *et al*., 2022). FTIR spectra of M–BC and KOH–M–BC surface were collected (Figure 6) and It can be observed that the band at 3907 cm^{-1}, 1563 cm^{-1} and 1000 cm^{-1} of M–BC could be attributed to vibrations of –OH, C=O and COO–, respectively (Lin *et al*., 2017). In case of KOH–M–BC the peaks were observed at 3315 cm^{-1} (–OH), 1562 cm^{-1} (C=O) and 1038 cm^{-1} (COO–) that show obvious change after modification, which could be due to KOH presence, resulting in abundant surface functional groups particularly –OH groups (Li *et al*., 2023). It is well believed that these functional groups are mainly responsible for adsorption that make a complex with Cr(VI) on biochar surface. This was previously described by Shi *et al*. (2020).

Table 1: Kinetic modeling parameters values for biochars.

First order			Second Order		
M–BC					
q_e (mg g^{-1})	k_1 (min^{-1})	R^2	q_e (mg g^{-1})	k_2 (g mg^{-1} min^{-1})	R^2
7.94	0.0052	0.76	76	0.008	0.99
KOH–M–BC					
q_e (mg g^{-1})	k_1 (min^{-1})	R^2	q_e (mg g^{-1})	k_2 (g mg^{-1} min^{-1})	R^2
11.74	0.0057	0.83	50	0.0083	0.99

Table 2: Isotherm modeling parameters values for biochars.

Langmuir	R^2	0.98
	K_L	0.12 (L g^{-1})
	Q_L	222 (mg g^{-1})
Freundlich	R^2	0.98
	K_L	0.22 (L g^{-1})
	Q_F	1.83 (mg^{1-n} g^{-1} L^n)
	R^2	0.78
	N	1.26

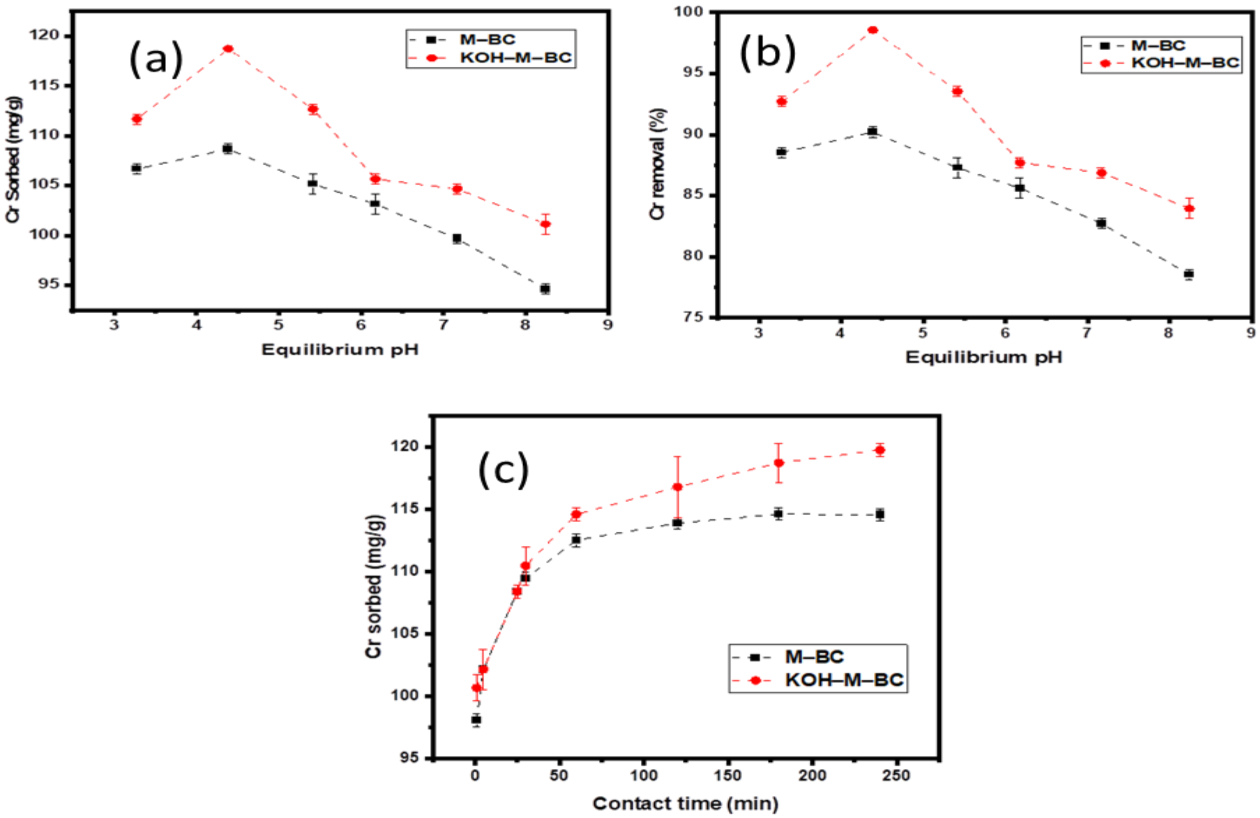

Figure 1. Sorption of Cr(VI) under varying pH (a, b) and contact time (c) environment by M–BC and KOH–M–BC

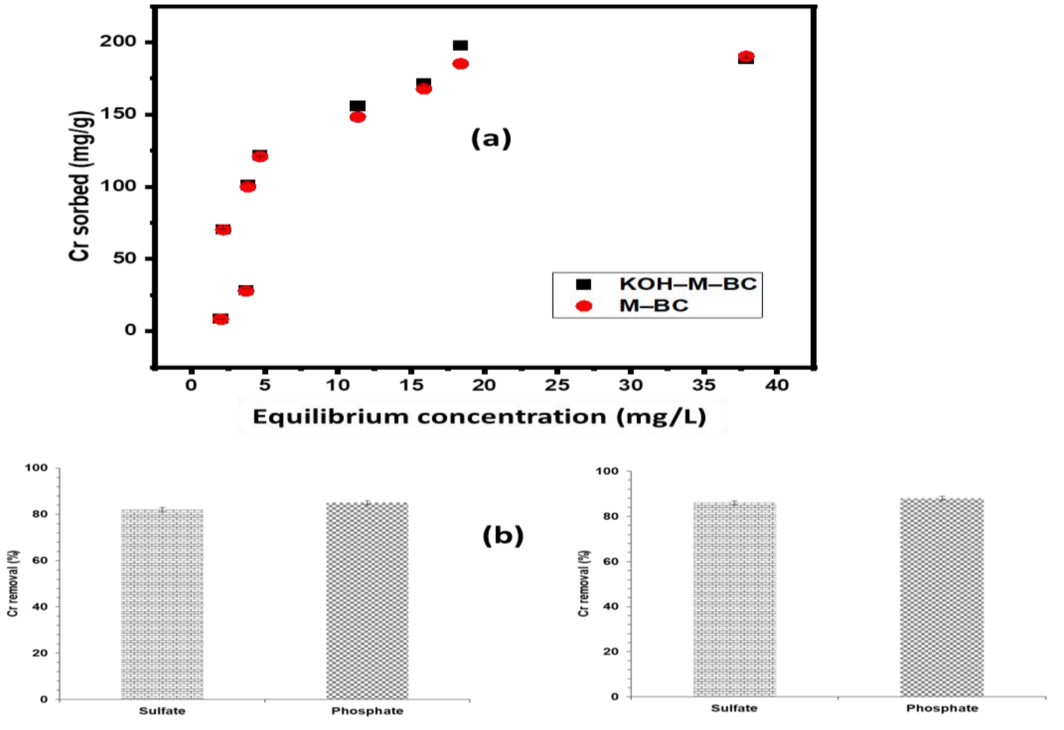

M–BC **KOH–M–BC**

Figure 2. Sorption of Cr(VI) under varying initial Cr(VI) (a) Effect of anions on Cr(VI) sorption by M–BC and KOH–M–BC (b)

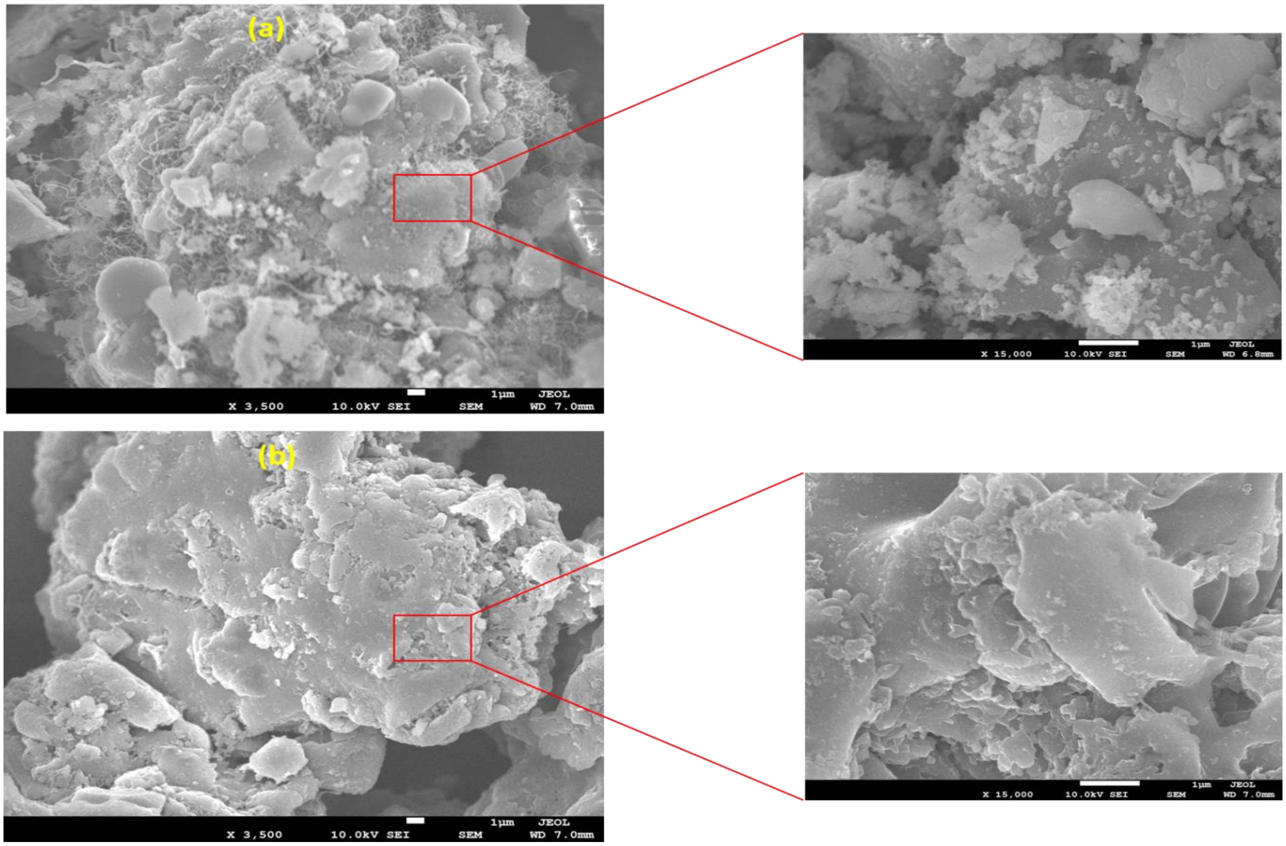

Figure 3. SEM analyses of (a) M–BC and (b) KOH–M–BC

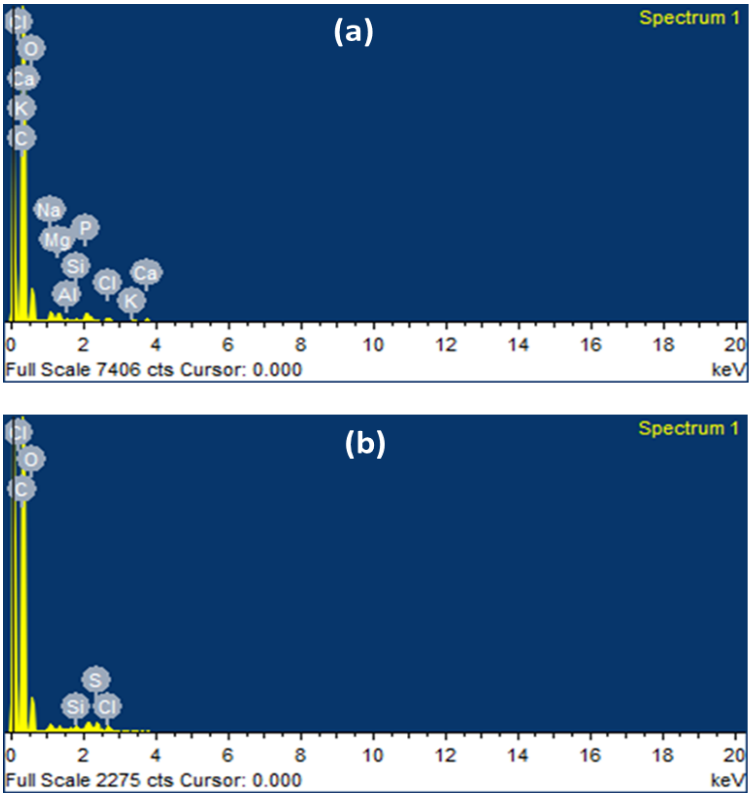

Element	Weight (%)	Atomic (%)
C K	78.59	85.35
O K	14.36	11.71
Na K	0.91	0.51
Mg K	0.82	0.44
Al K	0.19	0.09
Si K	0.34	0.16
P K	1.22	0.51
Cl K	1.18	0.43
K K	0.90	0.30
Ca K	1.48	0.48
Totals	100.00	

Element	Weight %	Atomic %
C K	79.33	85.15
O K	16.25	13.09
Si K	0.61	0.28
S K	2.40	0.97
Cl K	1.41	0.51
Totals	100.00	

Figure 4. EDS analyses of (a) M–BC and (b) KOH–M–BC

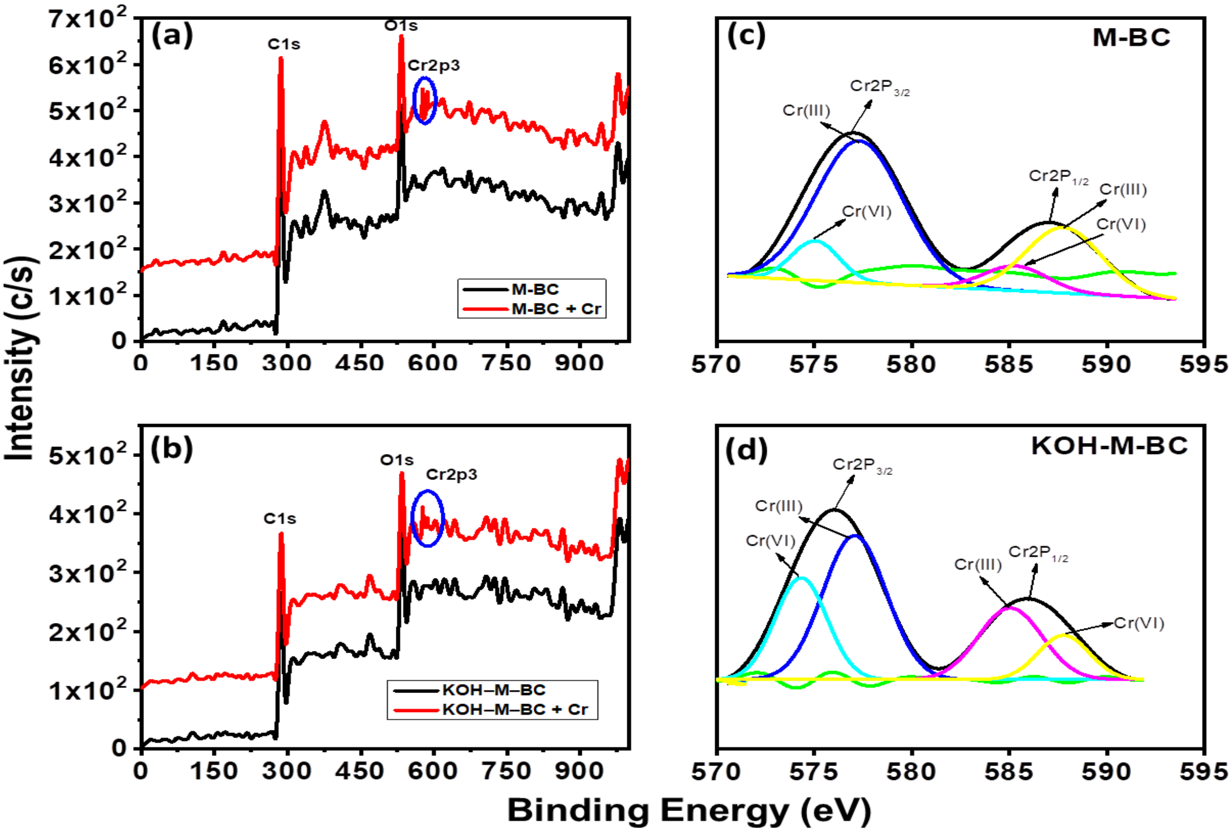

Figure 5. XPS survey scan of Cr(VI) adsorption onto (a) M–BC and (b) KOH–M–BC; The Cr2p spectra of (c) M-BC and (d) KOH-M-BC

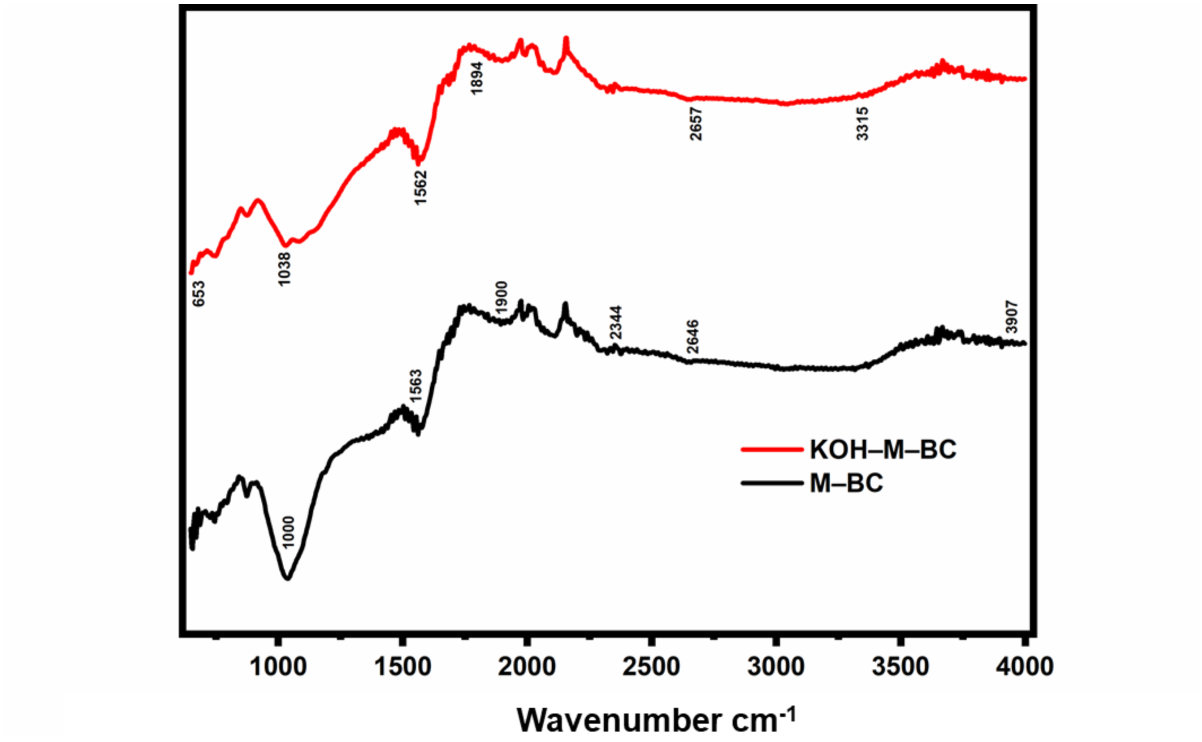

Figure 6. FTIR spectra of M–BC and KOH–M–BC for Cr(VI) sorption from water.

Conclusion: The combined hydrothermal carbonization of mosambi peel biocahr (M–BC) and modified alkali based KOH–M–BC is simple as an efficient method for sorption of Cr(VI) from water. The combined hydrothermal carbonization temperature was 450 °C and high sorption of Cr(VI) on modified KOH–M–BC sorbent (at pH 4, 118.7 mg/g (98.5%)) was obtained. The R^2 value for pseudo-second-order is higher (R^2 = 0.99) showing that this is best fitted model for Cr(VI) sorption in this study. Kinetic and isotherm models showed that chemisorption is dominant process for Cr(VI) sorption on KOH–M–BC sorbents. The SEM data showed that KOH–M–BC possessed a porous and highly wrinkled surface with many pore spaces. The XPS and FTIR results also confirmed the presence of O–rich surface functional groups and efficient Cr(VI) adsorption onto KOH–M–BC. The environmental friendly, low cost and viable organic material (mosambi peel biochar) can be used as potential biosorbent with future direction towards in filtration system and possible substitute to expensive inorganic filters for Cr(VI) removal from water.

Acknowledgments: The authors are thankful to University of the Punjab, Lahore, Pakistan for providing analytical facilities and financial support.

Competing Interests: All authors declare no conflict of interests.

REFERENCES

Ai, D., Tang, Y., Yang, R., Meng, Y., Wei, T., Wang, B., 2023. Hexavalent chromium (Cr(VI)) removal by ball-milled iron-sulfur @biochar based on P-recovery: Enhancement effect and synergy mechanism. Bioresource Technology 371, 128598.

Alghamdi, A.G., Ahmad, J., Alasmari, Z., Ibrahim, H.M., 2023. Removal of hexavalent chromium from contaminated soil and water by Mg/Fe layered double hydroxide and its composite with biochar. Arabian Journal of Geosciences 16(3), 145.

Basu, A., Saha, D., Saha, R., Ghosh, T., Saha, B., 2014. A review on sources, toxicity and remediation technologies for removing arsenic from drinking water. Res. Chem. Intermed. 40(2), 447-485.

Belachew, N., Hinsene, H., 2019. Preparation of cationic surfactant-modified kaolin for enhanced adsorption of hexavalent chromium from aqueous solution. Applied Water Science 10(1), 38.

Campos, A.F.C., de Oliveira, H.A.L., da Silva, F.N., da Silva, F.G., Coppola, P., Aquino, R., Mezzi, A., Depeyrot, J., 2019. Core-Shell Bimagnetic Nanoadsorbents for Hexavalent Chromium Removal from Aqueous Solutions. Journal of Hazardous Materials 362, 82-91.

Din, S.U., Khan, M.S., Hussain, S., Imran, M., Haq, S., Hafeez, M., Zain ul, A., Rehman, F.U., Chen, X., 2021. Adsorptive Mechanism of Chromium Adsorption on Siltstone–Nanomagnetite–Biochar Composite. Journal of Inorganic and Organometallic Polymers and Materials 31(4), 1608-1620.

Hu, L., Wang, P., Zhang, G., Liu, G., Li, Y., Shen, T., Crittenden, J.C., 2020. Enhanced persulfate oxidation of organic pollutants and removal of total organic carbons using natural magnetite and microwave irradiation. Chemical Engineering Journal 383, 123140.

Khalil, U., Bilal Shakoor, M., Ali, S., Rizwan, M., Nasser Alyemeni, M., Wijaya, L., 2020. Adsorption-reduction performance of tea waste and rice husk biochars for Cr(VI) elimination from wastewater. Journal of Saudi Chemical Society 24(11), 799-810.

Khalil, U., Shakoor, M.B., Ali, S., Rizwan, M., 2018. Tea waste as a potential biowaste for removal of hexavalent chromium from wastewater: equilibrium and kinetic studies. Arabian Journal of Geosciences 11, 1-9.

Kokab, T., Ashraf, H.S., Shakoor, M.B., Jilani, A., Ahmad, S.R., Majid, M., Ali, S., Farid, N., Alghamdi, R.A., Al-Quwaie, D.A., 2021. Effective removal of Cr (Vi) from wastewater using biochar derived from walnut shell. International Journal of Environmental Research and Public Health 18(18), 9670.

Li, Z., Wang, J., Chen, H., Wang, R., Zhu, M., 2023. Synthesis of ZnO Nanorod-Decorated Graphene Oxide for Application in Dental Resin Composites. ACS Biomaterials Science & Engineering 9(5), 2706-2715.

Lin, L., Qiu, W., Wang, D., Huang, Q., Song, Z., Chau, H.W., 2017. Arsenic removal in aqueous solution by a novel Fe-Mn modified biochar composite: Characterization and mechanism. Ecotoxicology and Environmental Safety 144, 514-521.

Masood ul Hasan, I., Javed, H., Hussain, M.M., Shakoor, M.B., Bibi, I., Shahid, M., Farwa, Xu, N., Wei, Q., Qiao, J., 2022. Biochar/nano-zerovalent zinc-based materials for arsenic removal from contaminated water. International journal of phytoremediation, 1-10.

Park, D., Yun, Y.-S., Lee, H.W., Park, J.M., 2008. Advanced kinetic model of the Cr(VI) removal by biomaterials at various pHs and temperatures. Bioresource Technology 99(5), 1141-1147.

Peng, H., Guo, J., 2020. Removal of chromium from wastewater by membrane filtration, chemical precipitation, ion exchange, adsorption electrocoagulation, electrochemical reduction, electrodialysis, electrodeionization, photocatalysis and nanotechnology: a review. Environmental Chemistry Letters 18(6), 2055-2068.

Prasad, K.S., Ramanathan, A., Paul, J., Subramanian, V., Prasad, R., 2012. Biosorption of arsenite (As+ 3) and arsenate (As+ 5) from aqueous solution by Arthrobacter sp. biomass. Environmental technology 34(19), 2701-2708.

Qu, J., Meng, X., Zhang, Y., Meng, Q., Tao, Y., Hu, Q., Jiang, X., You, H., Shoemaker, C.A., 2019. A combined system of microwave-functionalized rice husk and poly-aluminium chloride for trace cadmium-contaminated source water purification: Exploration of removal efficiency and mechanism. Journal of hazardous materials 379, 120804.

Qu, J., Wang, Y., Tian, X., Jiang, Z., Deng, F., Tao, Y., Jiang, Q., Wang, L., Zhang, Y., 2021. KOH-activated porous biochar with high specific surface area for adsorptive removal of chromium (VI) and naphthalene from water: Affecting factors, mechanisms and reusability exploration. Journal of Hazardous Materials 401, 123292.

Regmi, P., Moscoso, J.L.G., Kumar, S., Cao, X., Mao, J., Schafran, G., 2012. Removal of copper and cadmium from aqueous solution using switchgrass biochar produced via hydrothermal carbonization process. Journal of environmental management 109, 61-69.

Scharf, B., Clement, C.C., Zolla, V., Perino, G., Yan, B., Elci, S.G., Purdue, E., Goldring, S., Macaluso, F., Cobelli, N., 2014. Molecular analysis of chromium and cobalt-related toxicity. Scientific reports 4(1), 5729.

Shi, Y., Shan, R., Lu, L., Yuan, H., Jiang, H., Zhang, Y., Chen, Y., 2020. High-efficiency removal of Cr(VI) by modified biochar derived from glue residue. Journal of Cleaner Production 254, 119935.

Xue, Y., Gao, B., Yao, Y., Inyang, M., Zhang, M., Zimmerman, A.R., Ro, K.S., 2012. Hydrogen peroxide modification enhances the ability of biochar (hydrochar) produced from hydrothermal carbonization of peanut hull to remove aqueous heavy metals: batch and column tests. Chemical Engineering Journal 200, 673-680.

Zhang, X., Zhang, L., Li, A., 2018. Eucalyptus sawdust derived biochar generated by combining the hydrothermal carbonization and low concentration KOH modification for hexavalent chromium removal. Journal of Environmental Management 206, 989-998.

Zhao, N., Zhao, C., Lv, Y., Zhang, W., Du, Y., Hao, Z., Zhang, J., 2017. Adsorption and coadsorption mechanisms of Cr (VI) and organic contaminants on H3PO4 treated biochar. Chemosphere 186, 422-429.